
**AFRL-RX-WP-JA-2017-0528**

# SELECTIVE LASER MELTING FOR THE PREPARATION OF ULTRA-HIGH TEMPERATURE CERAMIC COATINGS (PREPRINT)

**Derek. King, Kathleen. Cissel, and Thomas. Key**
**UES, Inc.**

**Carmen Carney**
**AFRL/RX**

**John Middendorf**
**Universal Technology Corporaton**

**21 December 2017**
**Interim Report**



**(STINFO COPY)**

**AIR FORCE RESEARCH LABORATORY**
**MATERIALS AND MANUFACTURING DIRECTORATE**
**WRIGHT-PATTERSON AIR FORCE BASE, OH 45433-7750**
**AIR FORCE MATERIEL COMMAND**
**UNITED STATES AIR FORCE**

# REPORT DOCUMENTATION PAGE

*Form Approved*
*OMB No. 0704-0188*



| 1. REPORT DATE *(DD-MM-YY)* | 2. REPORT TYPE | 3. DATES COVERED *(From - To)* |
|---|---|---|
| 21 December 2017 | Interim | 9 July 2013 – 21 November 2017 |

**4. TITLE AND SUBTITLE**
SELECTIVE LASER MELTING FOR THE PREPARATION OF ULTRA-HIGH TEMPERATURE CERAMIC COATINGS (PREPRINT)

**5a. CONTRACT NUMBER**
FA8650-13-C-5207

**5b. GRANT NUMBER**

**5c. PROGRAM ELEMENT NUMBER**
63112F

**6. AUTHOR(S)**
1) Derek. King, Kathleen. Cissel, and Thomas. Key – UES
2) Carmen Carney – AFRL/RX
(continued on page 2)

**5d. PROJECT NUMBER**
3946

**5e. TASK NUMBER**

**5f. WORK UNIT NUMBER**
X0M4

**7. PERFORMING ORGANIZATION NAME(S) AND ADDRESS(ES)**
1) UES, Inc.
4401 Dayton-Xenia Rd,
Dayton, OH 45432
2) AFRL/RX
Wright-Patterson AFB, OH 45433
(continued on page 2)

**8. PERFORMING ORGANIZATION REPORT NUMBER**

**9. SPONSORING/MONITORING AGENCY NAME(S) AND ADDRESS(ES)**
Air Force Research Laboratory
Materials and Manufacturing Directorate
Wright-Patterson Air Force Base, OH 45433-7750
Air Force Materiel Command
United States Air Force

**10. SPONSORING/MONITORING AGENCY ACRONYM(S)**
AFRL/RXCC

**11. SPONSORING/MONITORING AGENCY REPORT NUMBER(S)**
AFRL-RX-WP-JA-2017-0528

**12. DISTRIBUTION/AVAILABILITY STATEMENT**
Distribution Statement A. Approved for public release: distribution unlimited.

**13. SUPPLEMENTARY NOTES**
PA Case Number: 88ABW-2017-6402; Clearance Date: 21 Dec 2017. This document contains color. The U.S. Government is joint author of the work and has the right to use, modify, reproduce, release, perform, display, or disclose the work.

**14. ABSTRACT *(Maximum 200 words)***
Results of selective laser melting of ultra-high temperature ceramic powders are presented. A powder blend of ZrB2, ZrC, and B4C was chosen to explore the impact of eutectic formation on the ability to prepare dense ceramic coatings on a metallic tungsten substrate using additive manufacturing methods. Laser powers between 200 and 400W were used for the application of the ceramic coatings. Analysis of the microstructure and composition of the resulting coatings was used to elucidate the effects thermal gradients and tungsten and SiC impurities had on the solidification of the ceramic coatings. To the authors' knowledge, these are the first ultra-high temperature ceramic coatings fabricated with a scanning laser melting process.

**15. SUBJECT TERMS**
ZrB2; ZrC; B4C SiC; silicon carbide; SiC-$HfB_2$; $SiO_2$; tungsten substrate; ceramic coating

| 16. SECURITY CLASSIFICATION OF: | | | 17. LIMITATION OF ABSTRACT: | 18. NUMBER OF PAGES | 19a. NAME OF RESPONSIBLE PERSON (Monitor) |
|---|---|---|---|---|---|
| a. REPORT | b. ABSTRACT | c. THIS PAGE | | | Carmen Carney |
| Unclassified | Unclassified | Unclassified | SAR | 14 | 19b. TELEPHONE NUMBER *(Include Area Code)* (937) 255-9154 |

# REPORT DOCUMENTATION PAGE Cont'd

**6. AUTHOR(S)**

3) John Middendorf - UTC

**7. PERFORMING ORGANIZATION NAME(S) AND ADDRESS(ES)**

3) Universal Technology Corporation
1270 N Fairfield Rd, Dayton, OH 45432

**Selective Laser Melting for the Preparation of Ultra-High Temperature Ceramic Coatings**

Carmen. Carney[1], Derek. King[1,2], John. Middendorf[3], Kathleen. Cissel[1,2], and Thomas. Key[1,2]

[1]*Materials and Manufacturing Directorate, Air Force Research Laboratory, WPAFB, OH, USA*

[2]*UES, Inc. Dayton, OH, USA*

[3] *UTC, Dayton, OH, USA*

**Abstract**

Results of selective laser melting of ultra-high temperature ceramic powders are presented. A powder blend of $ZrB_2$, ZrC, and $B_4C$ was chosen to explore the impact of eutectic formation on the ability to prepare dense ceramic coatings on a metallic tungsten substrate using additive manufacturing methods. Laser powers between 200 and 400W were used for the application of the ceramic coatings. Analysis of the microstructure and composition of the resulting coatings was used to elucidate the effects thermal gradients and tungsten and SiC impurities had on the solidification of the ceramic coatings. To the authors' knowledge, these are the first ultra-high temperature ceramic coatings fabricated with a scanning laser melting process.

**Introduction**

The demand for materials that sustain extreme thermal and chemical environments, encountered for applications such as hypersonic flight, aeropropulsion, and protection of reentry vehicles, has led to great interest in ultra-high temperature ceramics (UHTC). The class of UHTCs typically consists of transition metal borides, carbides, and nitrides, and are also recognized to have melting temperatures at or above 3000°C.[1-3] Like many monolithic ceramics, UHTCs are hard and chemically resistant, while also exhibiting unique thermal and electronic conductivity properties.[4] When exposed to an oxygen containing environment at temperatures in excess of 500-900°C, high temperature oxide scales will form that can resist

further oxidation, making UHTCs attractive environmental barrier coating options for metal alloys or ceramic matrix composites.[3,5]

Selective laser sintering (SLS) and selective laser melting (SLM) are rapid prototyping techniques that build materials layer by layer from powders and have been typically paired with the additive manufacturing of refractory metals and their alloys.[6-9] SLM is distinguished from SLS as a technique due to the melting of the powders compared to simply applying enough thermal energy to promote sintering of the powder particles. These techniques offer a promising method to fabricate coating or cladding layers of UHTCs with tailored microstructures and compositions. SLS has been used to sinter $ZrB_2$ powders with[10-12] and without binders[13]. In order to achieve full density, the SLS techniques utilized a binder phase such that the binder phase was either burned out during sintering or was a high temperature metallic, resulting in a cermet after an additional sintering step. Other additive manufacturing techniques, such as electron beam heating, were shown to melt $ZrB_2$, giving rise to large grain sizes and amorphous content that were dependent on the beam scan speed and current.[14]

An area of open research is the selection of UHTC compositions that will result in a fully dense ceramic coating using the SLM processes. UHTC eutectic combinations offer lower melting temperatures that could lead to a larger processing range with laser melting. Coatings resulting from solidified eutectics will have an array of microstructures that are dependent on the chosen composition and manufacturing parameters.[15-18] With this study we demonstrate the promise of using SLM to prepare adherent UHTC coatings on a W substrate and explore the final composition and microstructure of the resulting coatings.

**Experimental**

A powder blend of 38 vol%/43.4 wt% $ZrB_2$ (Grade B; H.C. Starck), 23.2 vol%/45.8 wt% ZrC (-325 mesh, 99.5%; Alfa Aesar), and 38.8 vol%/ 10.8 wt% $B_4C$ (-270 mesh, 99.5%; Cerac) was milled in ethanol with SiC grinding media in an attrition mill for 1 hr. The milled powder slurry

was subsequently dried using a rotary evaporator to remove the solvent and sieved to -80 mesh to break up agglomerates.

The SLM unit used was composed of a traditional two-platter powder spreading system coupled to a high power laser and was developed by Universal Technology Corporation (UTC, Dayton OH). The laser was an IPG YLR-500-SM, a 500 W maximum power, 1064 nm wavelength, continuous-wave laser with adjustable power from 10% to 100% (50 W-500 W). The powder bed was housed in a chamber which was filled with 99.9% argon gas during the processing. A flat blade was used to transfer UHTC powder from the supply reservoir to a tungsten (W) build platter in 50 µm layers. The laser beam was directed and focused on the sintering area using a galvonometer scanhead (to control x-y motion) coupled to a 6-inch focal length fused-silica F-theta lens. The galvonometer was computer controlled and used to print square coatings, nominally 10 mm by 10 mm. Other process parameters included scan line pitch of 60 µm and a scan speed of 500 mm/s. SLM trials were conducted with laser powers of 200, 250, 300, 350 and 400 W, producing adherent UHTC coatings in all cases; the results presented in this paper will focus on coatings processed with the 400 W laser which was shown to produce the most adherent and uniform coating.

X-ray diffraction (XRD) was performed on the parent $ZrB_2$-ZrC-$B_4C$ powder and the resulting coatings. Coupled $2\theta$ measurements were conducted in parallel beam mode using a Rigaku Ultima IV x-ray diffractometer with a Cu-k$\alpha$ source. Parallel beam mode was chosen to minimize the effect of sample roughness and eliminate peak shifts due to sample displacement from the Bragg plane. The coating was cut along the printed square diagonal, mounted in epoxy, and polished to a 1 µm mirror finish using successively finer diamond slurries. Cross sections of the post-processed coatings and starting powder were examined using scanning electron microscopy (SEM, Zeiss GeminiSEM 500, Jena, Germany) and electron dispersive spectroscopy (EDS, Oxford XMax Extreme, Abingdon, United Kingdom). All samples for

microscopy analysis were coated with a thin chromium layer to avoid charging and EDS peak overlaps.

**Results and Discussion**

Based on the Zr-C-B phase diagram,[19] the resulting coating was expected to contain $ZrB_2$, ZrC, and C, based on the starting powders. After attrition milling, $ZrB_2$, ZrC, $B_4C$, and SiC were observed via electron microscopy of the batched parent powder (Figure 1). The presence of SiC was confirmed as β-SiC, by XRD (not shown), and was determined to be an impurity from the SiC grinding media used for attrition milling. After printing, peaks for $ZrB_2$ (B), ZrC (C), W (W), and β-SiC (S) were identified in the parallel beam XRD analysis (Figure 2) of the coating. The broad peak located at ~25.8° was consistent with the presence of C. The W peak was determined to be a result of sampling the substrate and coating simultaneously.

A stitched optical micrograph of the 400 W coating diagonal cross-section is presented in Figure 3. Horizontal cracks were present in the W substrate and vertical cracks were present in the UHTC coating. It is possible that fracture occurred due to the thermal stresses caused by the difference in coefficient of thermal expansion of the UHTC coating (nominally $7 \cdot 10^{-6}$ $K^{-1}$) and the W substrate ($4.5 \cdot 10^{-6}$ $K^{-1}$). Before cutting, the coating appeared intact and the observed damage of the coating and substrate could have occurred during sectioning of the specimen due the development of such thermal residual stresses. The coating varied in thickness, and was measured to be ~380 µm at its thickest. Thickness non-uniformity was thought to partially be a result of using non-spherical particles, as irregular shaped particles (Figure 1) could have affected the layer deposition and particle packing density during printing. Previous literature on metallic SLS processes suggests that spherical grains, rather than irregular grains, tend to produce more homogeneous layer thicknesses,[20] due to better thermal conductivity between the particles.

In order to further investigate the microstructure, SEM images from various points through the thickness of the coating were examined. Figure 4 is an example of a location where acicular, needle-like, grains were present from the substrate interface (interface) to near the top of the coating. In the images taken from the interface and the middle of the coating, the acicular grains were well defined, with multiple phases located between grains. Qualitative point EDS analysis was conducted on the phases labeled in Figure 4 and these were shown to primarily consist of: (1) Zr-B, (2) Zr-C, (3) C, (4) Si-C, and (5) W. The W rich phases were often associated with an oxygen peak, suggesting these phases were an oxide. The incorporation of W into the coatings resulted from the melting of the W substrate. The W was shown to penetrate approximately 100 to150 µm into the coating. Delineation between the regions with and without W are shown in Figure 5a showing the impact of W on the grain morphology due to change in the solidification pathway. EDS analysis of the regions revealed the incorporation of W into the $ZrB_2$ grains in addition to the W-oxide phases (Figure 5b). Due to the increased complexity of the system, the coating solidification could not be evaluated through prior phase equilibria literature

The microstructure was also likely impacted by the local temperature. The first layers melted were close to the thick W substrate that could more effectively carry thermal energy away compared to the UHTC powder and coating, meaning that the thermal profile experienced by layers near the interface region would be different than surface layers further from the interface as they were being printed. It is hypothesized that near the interface, wicking of heat away from the melt lowered the temperature of the melt into a regime where high $ZrB_2$ nucleation and growth rates were favored. Moving toward the surface, removal of heat from the melt pool slows, as does the nucleation rate of $ZrB_2$. At the surface, heat from the laser is retained such that growth mechanisms become favored compared to $ZrB_2$ nucleation. This hypothesis was supported with microstructural observations; images ofthree regions taken at the same magnification, shown in Figure 4. Individual $ZrB_2$ grains were counted to number 262

at the substrate interface, 89 in the middle of the coating, and 54 at the top of the coating. Growth was also observed to change throughout the coating, where near the substrate, 52% of the grains fit within the bounds of the analyzed image. The number of counted grains that fit within the bounds of the imaged area dropped to 33% In the middle of the coating, and 20% at the surface. Overall, while the inclusion of W and SiC affected the intended solidification path, $ZrB_2$ could be identified as the phase of primary crystallization, where grain frequency and size elucidated the relative effect of temperature on the microstructure.

## Summary

In summary, a first of its kind UHTC coating was fabricated with an SLM process. A $ZrB_2$, ZrC, and $B_4C$ powder blend was prepared for the SLM fabrication of a $ZrB_2$, ZrC, C ternary eutectic UHTC coating. Ultimately, the incorporation of SiC and W, as impurities from the grinding media and substrate, dramatically impacted the crystallization and composition of the final coating. The successful fabrication of UHTC coatings, by SLM, demonstrated the ability to combine thermal composition considerations in order to control the morphology and composition of a coating printed directly onto a metallic substrate. Future work is planned to explore the processing variables to improve coating uniformity and density.

## References

1. Fahrenholtz W, Hilmas G, Talmy I, et al. Refractory diborides of zirconium and hafnium*. J Am Ceram Soc.* 2007;90:1347-1364.

2. Wuchina E, Opeka M, Causey S, et al. Designing for ultrahigh-temperature applications: The mechanical and thermal properties of HfB2, HfC x , HfN x and αHf(N). *J Mater Sci.* 2004;39:5939-5949.

3. Opeka M, Talmy I, Wuchina E, et al. Mechanical, thermal, and oxidation properties of refractory hafnium and zirconium Compounds*. J Euro Ceram Soc.* 1999;19:2405-2414.

4. McClane D, Fahrenholtz W, Hilmas G. Thermal properties of (Zr,TM)B2 solid solutions with TM = Hf, Nb, W, Ti, and Y*. J Am Ceram Soc.* 2014;97:1552-1558.

5. Parthasarathy T, Rapp R, Opeka M, et al. A model for the oxidation of $ZrB_2$, $HfB_2$ and $TiB_2$. Acta Mater. 2007;55:5999-6010.

6. Agarwala M, Bourell D, Beaman J, et al. Direct selective laser sintering of metals. *Rapid Prototyp J.* 1995;1:26-36.

7. Kruth J, Wang X, Laoui T, et al. Lasers and materials in selective laser sintering. *Assembly Automation.* 2003;23:357-371.

8. Yadroitsev I, Bertrand P, Smurov I. Parametric analysis of the selective laser melting process. *App Surf Sci*. 2007;253:8064-8069.

9. Osakada K, Shiomi M. Flexible manufacturing of metallic products by selective laser melting of powder. *Inter J Mach Tools Man*. 2006; 46:1188-1193.

10. Sun C., Gupta M, Payzant E. Effect of laser sintering on Ti–ZrB2 mixtures*. J Am Ceram Soc.* 2011; 94:3282-3285.

11. Sun C., Gupta M, Porter W. Thermophysical properties of laser-sintered Zr–ZrB2 cermets*. J Am Ceram Soc.* 2011;94:2592-2599.

12. Skripnyak V, Skripnyak E, Skripnyak V, et al. Simulation of mechanical properties of ceramic parts produced by additive technologies in a wide range of loading rates*.* In: Papadrakakis M, Papadopoulos V, Stefanou G, Plevris G, eds.Proceedings of the 2nd European Congress on Computational Methods in Applied Sciences and Engineering. Crete Island, Greece; 2016:341-354.

13. Sun C, Gupta M. Laser sintering of ZrB2*. J Am Ceram Soc.*2008;91:1729-1731.

14. Sun C, Gupta M, Taminger K. Electron beam sintering of zirconium diboride*. J Am Ceram Soc.* 2010;93:2484-2486.

15. Sorrell C, Stubican V, Bradt R. Mechanical properties of ZrC-ZrB2 and ZrC-TiB2 directionally solidified eutectics. *J Am Ceram Soc.* 1986;69:317-321.

16. Chen C, Zhou W, Zhang L. Oriented structure and crystallography of directionally solidified LaB6—ZrB2 eutectic. *J Am Ceram Soc.* 1998;81:237-240.

17. Tu R, Hirayama H, Goto T, Preparation of ZrB2-SiC composites by arc melting and their properties. *J Ceram Soc Japn.* 2008;116:431-435.

18. King D, Hilmas G, Fahrenholtz W. Plasma arc welding of ZrB 2–20vol% ZrC ceramics. *J Europ Ceram Soc.* 2014;34: 3549-3557.

19. Rudy E. Ternary phase equilibria in transition metal-boron-carbon-silicon systems. part 5. compendium of phase diagram data. AFML-TR-65-2; Aerojet-General Corp, Sacramento CA Materials Research Lab; 1969.

20. Olakanmi E, Cochrane R, Dalgarno K. A review on selective laser sintering/melting (SLS/SLM) of aluminium alloy powders: Processing, microstructure, and properties. Prog Mater Sci. 2015;74:401-477.

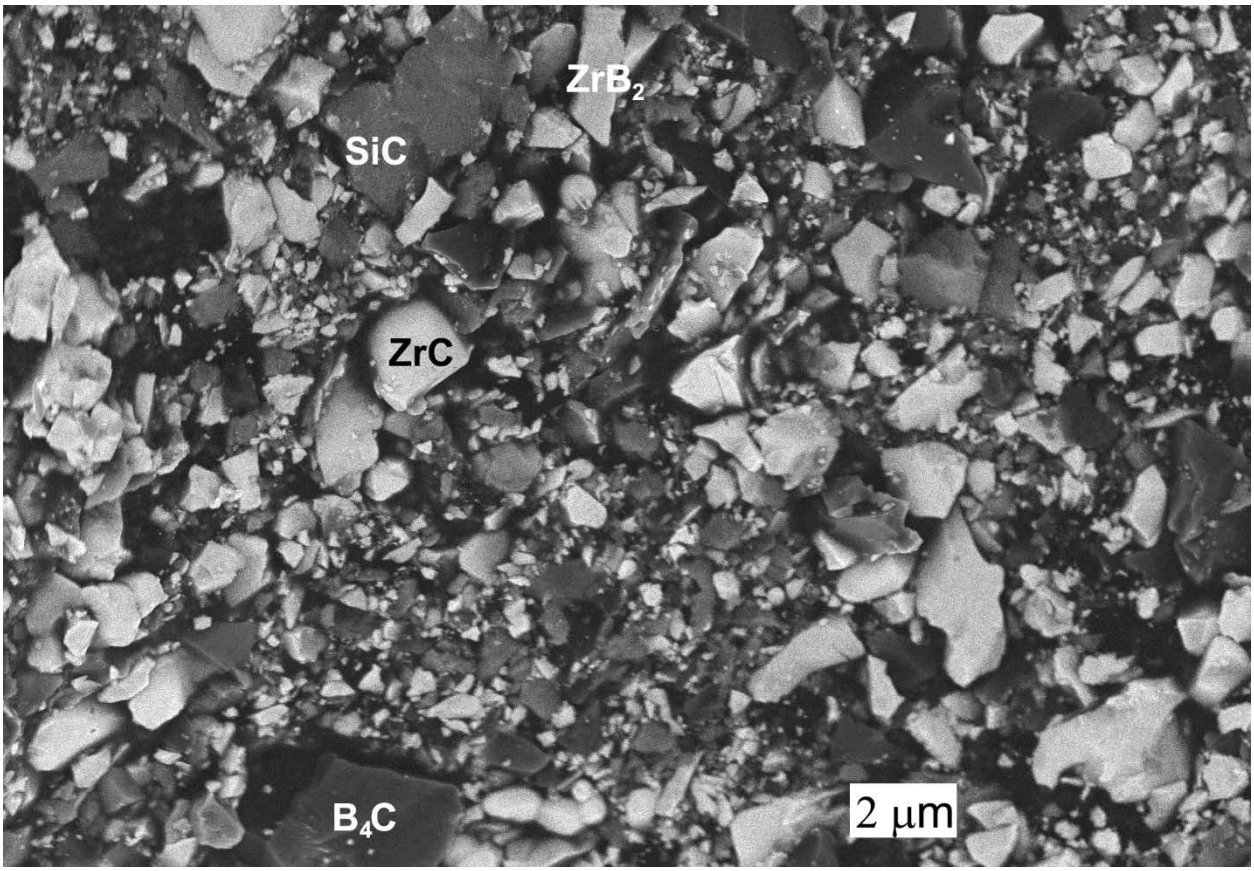


Figure 1. SEM micrograph of the powder morphology and composition. SiC was determined to be an impurity introduced by the attrition milling process.

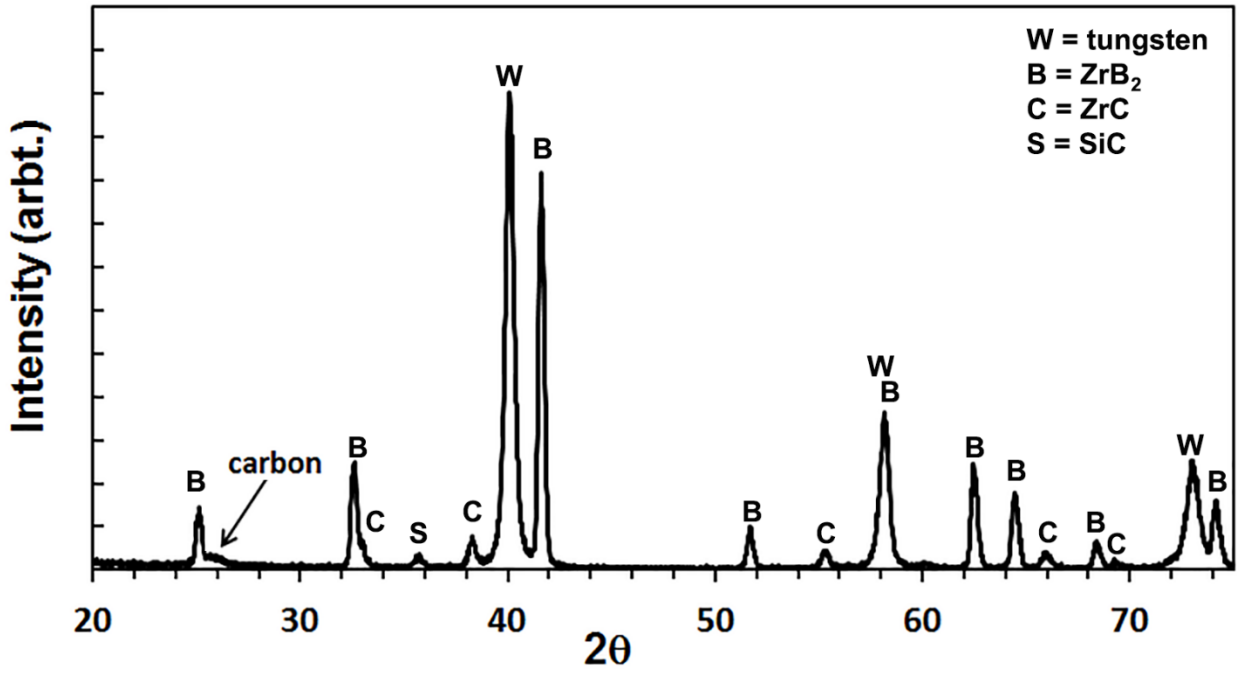


Figure 2. XRD pattern of the top surface of the coating after SLM. Peaks were identified as either $ZrB_2$, ZrC, SiC, or W. The broad shoulder at ~25.8° was attributed to carbon. In color online.

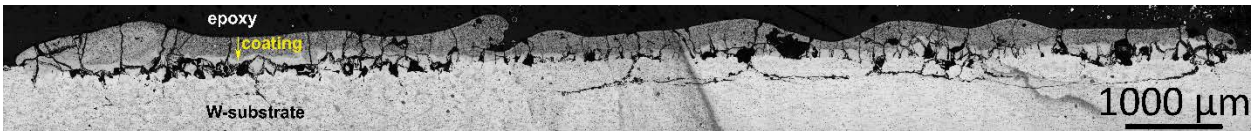


Figure 3. Optical Micrograph of the as-prepared UHTC coating using a 400 W laser power.

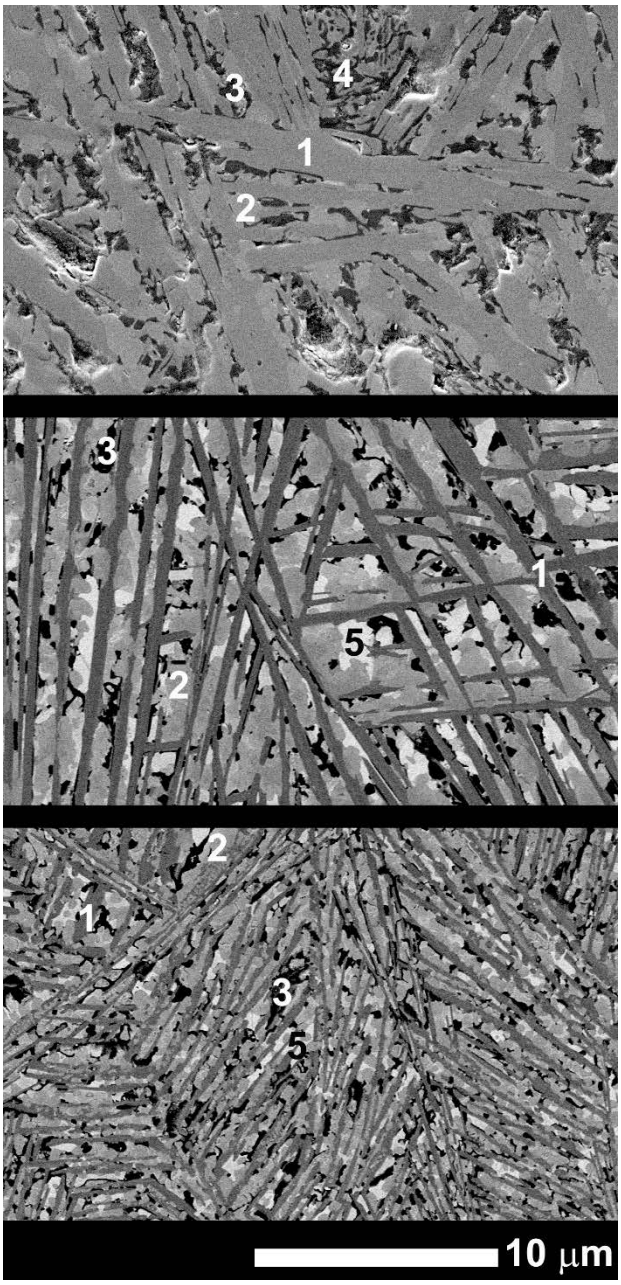


Figure 4. SEM micrographs showing the change in morphology from the top of the coating surface (top image) to the interface region (bottom image) for the coating processed using 400W. The phases were analyzed with EDS and are labeled (1) $ZrB_2$, (2) ZrC, (3) C, (4) C-Si, and (5) W-oxide accordingly.

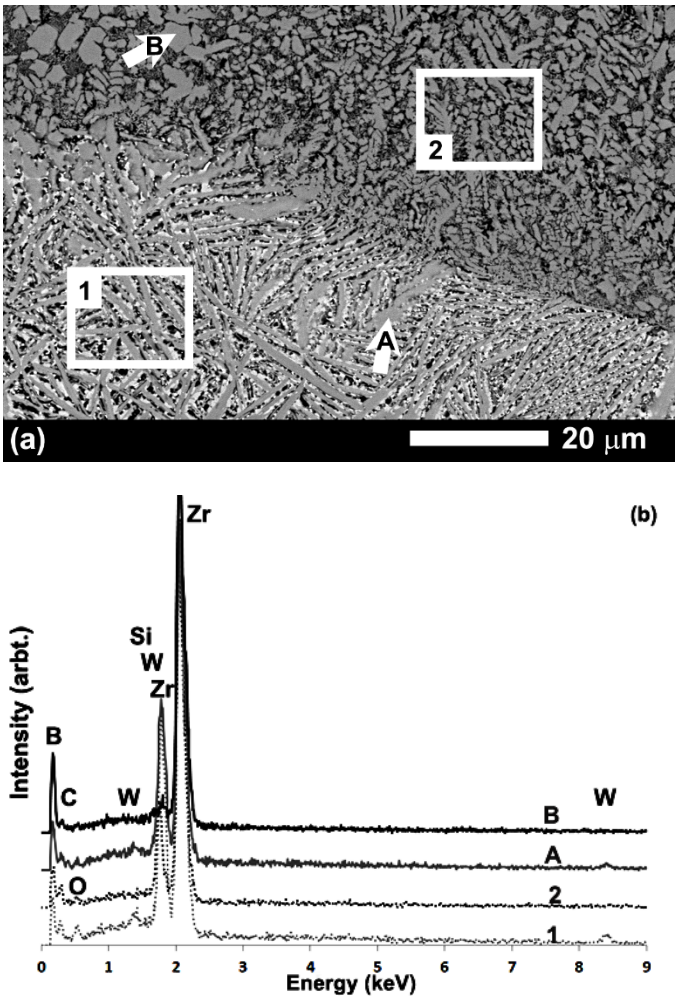


Figure 5. (a) BSE-SEM micrograph showing the transition from an acicular morphology and the location of W in the coating processed at 400W. (b) is the EDS analysis of the two boxed regions and the grains labeled A and B. The grey phases were $ZrB_2$ and ZrC, the dark phases were C, and Si-C, and the white phases were W containing.